

Immunotoxicity of Zinc Oxide (ZnO) Nanoparticles (NPs)

in vitro and in vivo

Hai-Duong Thi Nguyen

The Graduate School, Yonsei University

Department of Medicine

Immunotoxicity of Zinc Oxide (ZnO) Nanoparticles (NPs)

in vitro and *in vivo*

A Dissertation

Submitted to the Department of Medicine
and the Graduate School of Yonsei University
in partial fulfillment of the requirements
for the degree of Master of Medical Science

Hai-Duong Thi Nguyen

July 2012

**This certifies that the Master Dissertation of
Hai-Duong Thi Nguyen is approved**

Thesis supervisor: Prof. Soo-Ki Kim, MD, PhD

Committee member: Prof. Bae-Keun Park, PhD

Committee member: Maeng-Eun Ho, PhD

The Graduate School, Yonsei University

July 2012

AKNOWLEDGEMENTS

This thesis would not have been completed without the guidance and the help of several individuals who in one way or another contributed and extended their valuable assistance in the preparation and completion of this study.

Firstly, I would like to express my great debts of gratitude to my supervisor, Prof. Soo-Ki Kim, who gave me a great opportunity to do my graduate study in Korea. I sincerely appreciate his invaluable guidance, support, and inspiration in my research work. Special thank for his financial support in the last semester of my Master course.

I also would like to express my sincere gratitude to the members of my dissertation committee, including Prof. Bae-Keun Park, and Dr. Maeung-Eun Ho for their invaluable advice, support, and patience. In addition, I would like to specially thank to Prof. Jae-Min Oh, from Nano Bio Material Laboratory, Dept. of Chemistry and Medical Chemistry, Yonsei University for supporting me ZnO NP TEM photos, and his attribution for our nano-immunotoxicity study.

I would like to convey grateful thanks to Prof. Jun-Soo Park, from Molecular Cell Biology Laboratory, Division of Biological Science and Technology, Yonsei University for introducing me to my current supervisor. Without his help I may not do my graduate study in Korea.

I would like to thank Yonsei University for the Global Scholarship during my graduate study. I would like to acknowledge the members of Dept. of Microbiology, Wonju College of Medicine, Yonsei University: Prof. Joo-Young

Park, Prof. Kyong-Ho Lee, and Prof. Sun-Ju Choi for their concern and support. Special thanks to technicians and researchers: Cheol-Su Kim, Hyeon-Cheol Cho, Hyun-Sook Park, and other workers in the Dept. for their caring, guidance, and training.

I also would like to thank lecturers in Dept. of Microbiology and Infectious Disease, Faculty of Veterinary Medicine, Hanoi University of Agriculture: Prof. Quang Truong, Ha-Thai Truong, and Thanh-Huong Thi Chu for helpful suggestion to do research in the field of applied bio-medicine. Grateful thanks for their encouragement and support from undergraduate study up to now.

In my daily work I have been blessed with friendly and cheerful friends: Ma. Easter Joy Sajo and Rosa Mistica Coles Ignacio. Many thanks to Ranjan Das, Tuyet Nguyen, and other international friends for supporting and sharing the difficult time in research life with me. I also would like to convey many thanks to my dear friends: Kim-Lien T. Nguyen, Thu-Hien T. Nguyen, and other friends from TY49B and sincerely apologize that I could not mention one by one.

I feel a deep sense of gratitude to my parents and siblings for their unwavering love, encouragement, and understanding. Who always stand by me, and cheer me up through the good or bad times. Sincere thanks to my mother for understanding for me that during her difficult time I could not stay next to her, and my sisters for financial support. Thanks my younger brother for his caring. I warmly appreciate their generosity and understanding.

Finally, I would like to thank everybody who supported me for finishing the thesis, as well as express my apology that I could not mention personally one by one.

TABLE OF CONTENTS

ABSTRACT	1
I. INTRODUCTION	3
II. MATERIALS AND METHODS.....	6
1. <i>In vitro</i> experiment	6
1.1. Reagents.....	6
1.2. Characterization and preparation of ZnO NPs.....	6
1.3. Cell culture.....	7
1.4. CCK-8 cell viability assay.....	7
1.5. Impedance real-time cell viability (xCelligence).....	7
1.6. Detection of intracellular reactive oxygen species (ROS).....	8
1.7. Detection of changes in mitochondrial membrane potential (MMP).....	8
1.8. Detection of changes in antioxidant enzyme activity.....	9
2. <i>In vivo</i> experiment	9
2.1. Reagents.....	9
2.2. Maintenance of animals and ZnO NP treatment.....	10
2.3. Coefficient of spleen to body weight.....	10
2.4. Induction and evaluation of delayed-type hypersensitivity (DTH).....	10
2.5. Preparation of splenocytes.....	11
2.6. Splenocyte proliferative responses to concanavalin A, and lipopolysaccharide.....	11
2.7. Cytotoxicity assay of natural killer (NK) cells.....	12
2.8. Immunophenotyping of splenocytes.....	12
2.9. Measurement of nitric oxide (NO).....	13

2.10. Measurement of serum cytokine level.....	13
3. Statistical analysis.....	13
III. RESULTS.....	14
1. ZnO NP Preparation	14
1.1. Dispersion tests.....	14
1.2. Physicochemical characterizations of ZnO NPs.....	16
2. <i>In vitro</i> immunotoxicity.....	18
2.1. End-point cell viability.....	18
2.2. Real-time cell viability.....	21
2.3. ZnO NPs induce the generation of intracellular ROS in Raw 264.7 cells.....	23
2.4. Effect of ZnO NPs on mitochondrial membrane potential (MMP).....	25
2.5. Effect of ZnO NPs on antioxidant enzyme (SOD, GPx) activity..	27
3. <i>In vivo</i> immunotoxicity.....	29
3.1. Change of body weight and behavior.....	29
3.2. Spleen weight, and coefficient of spleen to body weight.....	31
3.3. Immunotoxicity parameters.....	33
3.3.1. Immunophenotyping	33
3.3.2. Innate, cell-mediated immune response (DTH and mitogenic response) against ZnO NPs	36
3.3.3. NO production of splenocytes.....	40
3.3.4. Serum cytokine level.....	42
IV. DISCUSSION	44
V. REFERENCES	50

LIST OF FIGURES

Fig.1	Digital images of ZnO NPs in three different aqueous solutions (PBS pH 7.4, L-Serine/HEPES pH 6.2, Citrate/HEPES pH 7.3), and ZnCl ₂ in PBS pH 7.4 before and after mixing with vortex for 5 min.....	15
Fig.2	Scanning electron microscopic images of ZnO NPs.....	17
Fig.3	Effect of ZnO NPs and ZnCl ₂ on the viability of Raw 264.7 cells.	19
Fig.4	Effect of ZnO NPs on real-time cell viability of Raw 264.7 cells..	22
Fig.5	Effect of ZnO NPs on intracellular ROS generation in Raw 264.7 cells.....	24
Fig.6	Effect of ZnO NPs on mitochondrial membrane potential (MMP) in Raw 264.7 cells.....	26
Fig.7	Effect of ZnO NPs on (a) superoxide dismutase (SOD), and (b) glutathione peroxidase (GPx) activity in Raw 264.7 cells.....	28
Fig.8	Body weight change of mice after ZnO NP administration.....	30
Fig.9	Effect of ZnO NPs on spleen weight (a), coefficient of spleen to body weight (b) after 14 day ZnO NP oral administration.....	32
Fig.10	Distribution of leukocytes from spleen after ZnO NPs oral administration for 14 days.....	34
Fig.11	Mitogenic response of mouse splenocytes.....	39
Fig.12	Nitric oxide (NO) production induced by ZnO NPs in mouse splenocytes.....	41
Fig.13	Serum cytokine profiles in ZnO NP-fed mice.....	43

LIST OF TABLES

Tab.1	EC ₅₀ values (24 h growth inhibition) of ZnO NPs and ZnCl ₂ on Raw 264.7 cells.....	20
Tab.2	Immunophenotype of splenocytes in C57BL/6 mice administered with ZnO NPs for 14 days.....	35
Tab.3	NK cell activity in ZnO NP-fed mice.....	37
Tab.4	Delayed-type hypersensitivity in ZnO NP-primed mice.....	38

ABSTRACT

Immunotoxicity of Zinc Oxide (ZnO) Nanoparticles (NPs)

in vitro and in vivo

Hai-Duong Thi Nguyen

Dept. of Medicine

The Graduate School

Yonsei University

While Zinc Oxide (ZnO) nanoparticle (NP) has been recognized to have promising applications in biomedicine, its immunotoxicity has been inconsistent and even contradictory. To address this issue, we investigated whether ZnO NPs with different sizes (20 nm or 100 nm) and electrostatic charges (negative or positive) would cause immunotoxicity *in vitro* and *in vivo*, and explored their underlying molecular mechanism. Using Raw 264.7 cell line, we examined cell viability, reactive oxygen species (ROS) generation, mitochondrial membrane potential (MMP), and antioxidant enzyme activity to explore the immunotoxicity

mechanism of ZnO NPs *in vitro*. We found that in cell viability assay (CCK-8, real-time xCelligence) ZnO NPs with different size and charge could induce differential cytotoxicity to Raw 264.7 cells. Specifically, the positively charged ZnO NPs exerted higher cytotoxicity than the negatively charged one. Molecular study to unravel the mechanism of immune cell toxicity showed that overall, treatment of ZnO NPs decreased MMP, generated intracellular ROS, and reduced antioxidant enzyme activity such as glutathione peroxidase (GPx). Next, to gauge systemic immunotoxicity, we assessed immune responses of C57BL/6 mice after orally administration of sub-lethal dose of ZnO NPs for two weeks. Oral intake of ZnO NPs significantly decreased body weight gain. In parallel, ZnO NPs did not alter the cell-mediated immune response in mice but suppressed innate immunity such as NK cell activity. The CD⁴⁺/CD⁸⁺ ratio was slightly reduced which implies the alteration of immune status induced by ZnO NPs. Accordingly, nitric oxide (NO) production from splenocyte culture supernatant in ZnO NP-fed mice was lower than control. Consistently, serum levels of pro/anti-inflammatory (IL-1, TNF- α , and IL-10) and Th1 cytokines (IFN- γ , IL-12) in ZnO NP-fed mice were significantly suppressed. Collectively, our results indicate that different sized- and charged-ZnO NPs would cause *in vitro* and *in vivo* immunotoxicity, of which nature is a minor immunosuppression. This has important implications for individuals who may be chronically exposed to ZnO NPs.

Key words: ZnO NPs, immunotoxicity, ROS, immunosuppression, size, charge.

I. INTRODUCTION

Nanotechnology has enabled NPs to be designed at the molecular (nanometer) level. Thus, NPs have received the tremendous advantage of their small size, novel physicochemical properties as well as their interactions with biological systems. In particular, inorganic NPs with metal oxides have been preclinically employed for the diagnostic and the therapeutic use in biomedicine (Duguet et al. 2006, 157-68, Salata 2004, 3, Sanvicens, and Marco 2008, 425-33, Zhang et al. 2008, 761-9). Of these metal oxides, ZnO NPs have received considerable attention with a promising biological application for drug delivery and cancer therapy (De Jong, and Borm 2008, 133-49, Hanley et al. 2008, 295103, Zhang et al. 2011, 1906-14) due to their great photocatalytic and photo-oxidizing ability against chemical and biological species.

Despite the potential bio-medical application of ZnO NPs, biohazards and toxicities of ZnO NPs remained unclear. Of these toxicities, the effects of ZnO NPs on immune system are poorly documented. Here, immunotoxicity is defined as the adverse effects on immune system such as hypersensitivity, chronic inflammation, immunosuppression, immunostimulation, and autoimmunity. Many evidences suggested that ZnO NPs would function as immunotoxicants (Hooper et al. 2011, 1111-7, Jang, Lim, and Choi 2010, 85-91, Matsumura et al. 2010, 232-7, Pasupuleti et al. 2011). ZnO NPs have unique physiochemical properties, therefore, they could easily access several immune tissues and cells through various routines such as inhalation, ingestion, skin uptake, and injection. ZnO NP oral administration could cause severe damages in heart, lung, liver, and kidney (Zheng, Li, and Wang 2009, 1566-1571),

consequently leading to complicated inflammation. Likewise, profuse release of inflammatory mediators induced by ZnO NPs (Heng et al. 2011, 1517-28, Roy et al. 2011, 110-1) may result in immune stimulation or aggravation of immune diseases (Yanagisawa et al. 2009, 314-22), or even break down Th1/Th2 balance (Liu et al. 2009, 3934-3945).

It is well known that immunotoxicity of NPs were intimately linked to oxidative stress. For instance, the toxicity of ZnO NP to immune cells was involved in ROS generation (Hanley et al. 2009, 1409-1420, Heng et al. 2010, 1762-6, Lipovsky et al. 2011, 105101, Song et al. 2010, 389-97). The high production of super oxide in mitochondrial reduced the mitochondrial membrane potential (Moos et al. 2010, 733-9), caused cell cycle arrest at S/G2 phase (Sasidharan et al. 2011, 3657-69), and increased the ratio of Bax/Bcl2 leading to mitochondria mediated pathway involved in apoptosis (Sharma, Anderson, and Dhawan 2012). But, the mechanism of immunotoxicity of ZnO NPs in relation to oxidative stress is unclear.

To trigger immunotoxicity, several traits of NPs such as size, shape, electrostatic charge are very essential (Di Gioacchino et al. 2011, 65S-71S). Emerging evidences implied that the toxicity of ZnO NPs could be affected by size and/or electrostatic charge (Sohaebuddin et al. 2010, Sun, Zhao, and Lombardi 2007, Yang et al. 2009, 69-78). For instance, increase of ZnO NPs size might conversely decrease their toxicities (Hanley et al. 2009, 1409-20, Padmavathy, and Vijayaraghavan 2008). Positively charged NPs could exert higher immunotoxicity than negatively charged NPs due to effective interaction with negative charge of acidic acid on surface of macrophage (P. D. Dwivedi et

al., 2009). However, these studies failed to address whether the immunotoxicity of ZnO NPs would be affected by the size and/or charge, if so, its immunotoxicity is immunostimulatory or immunosuppressive.

In this study, we explored the *in vitro* potential immunotoxicity of ZnO NP on Raw 264.7 cells, and the systemic *in vivo* immunotoxicity of ZnO NPs using C57BL/6 mice. Further, we investigated the role of size and charge in ZnO NP-induced immunotoxicity.

II. MATERIALS AND METHODS

1. *In vitro* experiment

1.1. Reagents

ZnO-310 was purchased from Sumitomo Osaka Cement Co. Ltd (Tokyo, Japan). Zn-OX-01-NP.100N was purchased from Amerian Elements (Los Angeles, USA). Dulbecco's Modified Eagle's Medium (DMEM), and fetal bovine serum (FBS) were obtained from Hyclone Laboratories, Inc. (South Logan, USA). Cell Counting Kit-8 (CCK-8) was from Dojindo Molecular Technologies, Inc. (Rockville, USA). Peroxide-sensitive fluorescent probe, 2,7-dichlorodihydrofluorescein diacetate (H₂DCFDA) was purchased from Sigma Chemical Co. (St Louis, USA). 5,5',6,6'-tetrachloro-1,1',3,3'-tetraethylbenzimidazolylcarbocyanine iodide (JC-1) was from Molecular Probes Inc. (Eugene, USA). SOD and GPx kit were from Biovision Inc. (Mountain View, USA). The normal physiological salt solution (NPSS) used throughout this study had the following composition (in mM) 125 NaCl, 4.7 KCl, 1.2 KH₂PO₄, 1.2 MgSO₄, 2.5 CaCl₂, 18 NaHCO₃, 0.026 Na₂EDTA, and 11.2 Glucose.

1.2. Characterization and preparation of ZnO NPs

The ZnO NPs used in this study were sized at 20 nm (ZnO-310, Sumitomo Osaka Cement Co. Ltd, Tokyo, Japan) and 100 nm (Amerian Elements, Los Angeles, USA) with approximately 99.5% purity, milky white color, nearly spherical shape. In brief, 20 mg dry powder of ZnO NPs was dissolved into 100 ml L-Serine/HEPES pH 6.2, and Citrate/HEPES pH 7.3 to make NP surface electrostatic charge. Indicated buffers were made as follows: for the positive charge buffer, 99 ml of 20 mM HEPES pH 6, L-Serine (1 g) adjusted to pH 6.2, and for the negative charge buffer, 99 ml of 20 mM HEPES

pH 7, Sodium Citrate (1 g) adjusted to pH 7.3. Subsequently, the ZnO NP suspension was vortexed for 5 min at room temperature then kept in 4 °C up to use. Before using the suspension was sonicated at 4 °C for 10 min with a sonicator (Hielscher-Ultrasound Technology, Teltow, Germany).

1.3. Cell culture

Raw 264.7, mouse macrophage cell line (American Type Cell Culture Collection) was maintained in DMEM (Hyclone Laboratories, Inc., South Logan, USA) supplemented with 10% heat-activated fetal bovine serum (FBS, Hyclone Laboratories Inc., South Logan, USA) and 1% Antibiotic-Antimycotic (Gibco, Invitrogen Corporation, Auckland, N.Z) at 37 °C in 5% CO₂ incubator.

1.4. CCK-8 cell viability assay

A commercial available cell viability assay Cell Counting Kit-8 (CCK-8, Dojindo Molecular Technologies, Inc., Rockville, USA) was employed to evaluate the cytotoxic effect of ZnO NPs. Approximately 1×10^5 of Raw 264.7 cells were seeded into each well of 96-well plates then incubated with various concentration of ZnO NPs for 24 h at 37 °C in a 5 % CO₂ incubator. Afterwards, 10 µl of CCK-8 solution was added to each well, incubated for 1 h, and then absorbance was determined at 450 nm by a DTX-880 multimode microplate reader (Bechman Counter Inc., Fullerton, USA).

1.5. Impedance real-time cell viability (xCelligence)

Impedance real-time cell viability was measured using xCelligence (ACEA Biosciences, San Diego, USA). Approximately 1×10^4 of Raw 264.7 cells were seeded into each well of 16-well electronic plates (E-Plate 16) to allow attachment and growth on the sensor of the E-Plate 16. ZnO NPs were prepared in DMEM and added into wells containing cells. Thereafter, the sensor devices

were mounted back to device stations placed inside a CO₂ incubator. Cell index (CI) was automatically recorded every 15-20 min continuously for 96 h by the RT-CES system to produce time dependent response dynamic curves.

1.6. Detection of intracellular reactive oxygen species (ROS)

The generation of intracellular reactive oxygen species (ROS) was monitored with peroxide-sensitive fluorescent probe, 2,7-dichlorodihydrofluorescein diacetate (H₂DCFDA) (Sigma Chemical Co., St. Louis, USA) according to the manufacture's guideline. Briefly, Raw 264.7 cells were seeded at approximately 2×10^4 cells per well in 96 well black plates for 12 h before treatment. Thereafter, cells were treated with 20 µg/ml of ZnO NPs for different indicated times (0.5, 1, 3, 6, 24 h) then washed with NPSS and loaded with 10 µM of H₂DCF-DA (Sigma Chemical Co., St Louis, USA) from a stock solution in DMSO. After a 30 min loading at 37 °C in dark incubator, cells were washed again with NPSS to remove extra H₂DCFH-DA, and immediately measured at an excitation wavelength of 485 nm and an emission wavelength of 530 nm using a DTX-880 multimode microplate reader (Bechman Counter Inc., Fullerton, USA).

1.7. Detection of changes in mitochondrial membrane potential (MMP)

Mitochondrial membrane potential (MMP) was determined using the lipophilic cationic probe: 5,5',6,6'-tetrachloro-1,1',3,3'-tetraethylbenzimidazolylcarbocyanine iodide (JC-1) (Molecular Probes Inc., Eugene, USA). Briefly, Raw 264.7 cells were seeded at approximately 2×10^4 cells per well in 96 well black plates for 12 h before treatment. Thereafter, cells were treated with 20 µg/ml of ZnO NPs for 3 h, washed once with NPSS, then loaded with 5 µM of JC-1 at 37 °C for 20 min. Cells were rinsed in NPSS twice

and assayed using a fluorescence spectrometer (Flex Station II 384, Molecular Devices Corp., Sunnyvale, USA). The fluorescence ratio (590 to 530 nm) was used for quantitative analysis.

1.8. Detection of changes in antioxidant enzyme activity

Activity of superoxide dismutase (SOD) and glutathione peroxidase (GPx) were measured using BioVision kit (Mountain View, USA). Briefly, Raw 264.7 cells were seeded at approximately 1×10^6 cells per dish in 60 mm dishes and treated with 20 $\mu\text{g/ml}$ of ZnO NPs for 3 h. After treating, the cells were washed once with PBS, scraped, lysed, and then centrifuged at 12,000 *rpm* for 15 min at 4 °C. The supernatant (cell lysate) was removed and the protein concentration was measured by the Bradford method. The activities of different antioxidant enzymes were then measured in the cell lysates following the instruction of the manufacturer.

2. *In vivo* experiment

2.1. Reagents

Lactase dehydrogenase (LDH) release cytotoxic assay, Griess reagent-G2930 were obtained from Promega Corp. (Madison, USA). Concanavaline A (ConA), lipopolysaccharide (LPS, derived from *Salmonella typhosa*), Hank's balanced salt solution (HBSS), and trypan blue were purchased from Sigma-Aldrich Co. (St. Louis, USA). Park Memorial Institute (RPMI) 1640 medium was obtained from Hyclone Laboratories, Inc. (Utah, USA). All monoclonals (CD4, CD8, CD19, B220, CD16, CD14, CD11) were purchased from BD Bioscience (San Diego, USA).

2.2. Maintenance of animals and ZnO NP treatment

Six-week-old inbred C57BL/6 mice (Orient Bio Co. Ltd., South Korea) were maintained in a pathogen-free condition, fed with a standard commercial diet. Mice were randomly assigned into five groups: negative control which was PBS treated, and four experimental groups were treated with four types of ZnO NPs. Briefly, ZnO NP suspension was orally administered into the mice with the dosage of 750 mg/kg every day continuously for 14 days. Mouse body weight was calculated every day. All experiments were performed according to the Animal Ethic Guidelines and were approved by the Institutional Animal Care and Use Committee (IACUC) at Wonju College of Medicine, Yonsei University, Wonju city, Kangwon province, South Korea.

2.3. Coefficient of spleen to body weight

Spleen was removed aseptically after sacrifice and weighed. The coefficient of spleen to body weight was calculated as the ratio of tissues (wet weight, mg) to body weight (BW) (g).

2.4. Induction and evaluation of delayed-type hypersensitivity (DTH)

Delayed-type hypersensitivity assays were performed 4 days before sacrifice. To assess DTH response, mice were subcutaneously injected left footpad with 20 μ l of Saline as a control, and into right footpad with 20 μ l of ZnO NPs suspension. At the indicated times after challenge (24 h and 48 h), footpad thickness was measured with a digital caliper (Mitutoyo Corporation, Tokyo, Japan). The level of the DTH response was determined as the difference between the left and right footpad.

2.5. Preparation of splenocytes

To isolate splenocytes, the spleen was removed aseptically from C57BL/6 mouse at the end point treatment and placed in Hank's balanced salt solution (HBSS, Sigma Chemical Co., St. Louis, USA). Splenocyte suspensions were prepared by gently pressing the spleen between the frosted ends of two sterile microscope slides into a 90 mm Petri dish. The slides were washed with RPMI-1640 medium (Hyclone Laboratories, Inc., South Logan, USA). Cell suspension were filtered by a sterile plastic strainer then centrifuged at 1500 *rpm* for 3 min. Thereafter, the cell pellets were washed three times in PBS and resuspended in RPMI-1640 supplemented with 3 % fetal bovine serum (FBS, Hyclone Laboratories Inc., South Logan, USA). The viability of the cells used in all experiments was always higher than 85%, as measured by trypan blue exclusion (Sigma Chemical Co., St Louis, USA).

2.6. Splenocyte proliferative responses to concanavalin A, and lipopolysaccharide

Splenocytes were seeded at 1×10^5 cells per well into 96 well-flat-bottom-plate in 100 μ l RPMI-1640 (Hyclone Laboratories, Inc., South Logan, USA) supplemented with 10% heat-activated FBS (Hyclone Laboratories Inc., South Logan, USA) and 1% antibiotic/antimycotics. Thereafter, concanavalin A (ConA, Sigma-Aldrich Co., St. Louis, USA) with 4 different concentrations (10, 5, 2.5, and 1.25 μ g/ml), or 100 μ g/ml of lipopolysaccharide (LPS, Sigma-Aldrich Co., St. Louis, USA) were utilized. The plates were incubated at 37 °C in a humidified atmosphere under 5% CO₂ for 48 h. Cell proliferation was evaluated using a CCK-8 kit (Dojindo Molecular Technologies, Inc., Rockville, USA).

2.7. Cytotoxicity assay of natural killer (NK) cells

Splenocytes (effector cells) were plated into 96 well-flat-bottom plates at 10^5 cells/well in 100 μ l RPMI-1640 (Hyclone Laboratories, Inc., South Logan, USA). YAC-1 cells (target cells, American Type Cell Culture Collection, Manassas, VA) were subcultured in RPMI-1640 medium supplemented with 10% FBS. After 24 h, splenocytes were incubated with YAC-1 at appropriate concentrations to obtain effector: target ratios of 100:1; 50:1; 25:1 for 6 h at 37 °C in atmosphere containing 5% CO₂. The cytotoxic activity of NK cells was assessed by a LDH release cytotoxic assay (Promega Corp., Madison, USA). LDH was assayed in the supernatant by optical density (OD) measurement at 490 nm. Target cell lysis was calculated as: $(\text{OD of sample} - \text{OD with spontaneous release of LDH from target cells} - \text{OD with spontaneous release of LDH from effector cells}) \times 100 / (\text{OD with maximal release of LDH from target cells} - \text{OD with spontaneous release of LDH from target cells})$.

2.8. Immunophenotyping of splenocytes

Specific leukocyte subtypes of cells derived from mouse spleen were also determined by immunofluorescent antibody staining and analyzed with flow cytometry. Lymphocyte subpopulations were identified and gated using forward versus side scatter characteristics. All monoclonals were directly conjugated and were obtained from BD Bioscience (San Diego, USA). T cells (CD4, CD8), B cells (CD19, B220), NK cells (CD16) and monocytes (CD14, CD11) were identified using the anti-mouse antibodies. Thereafter, approximately $3-5 \times 10^3$ cells were resuspended in flow cytometry buffer (2% FBS, 0.02% sodium azide in PBS) containing Fc-block to reduce non-specific antibody binding. Cells were then incubated in the dark with the appropriate fluorochrome-conjugated

antibody (10 μ l) for 30 min at 4 °C. Afterwards, cells were washed twice with 500 μ l FACS (Fluorescence Activated Cell Sorter) buffer and flow cytometry analysis was performed on the FACS Calibur system (BD Biosciences, Franklin Lakes, USA). Control samples were matched for each fluorochrome. Data were analyzed using CellQuest software (BD Biosciences, Franklin Lakes, USA).

2.9. Measurement of nitric oxide (NO)

NO production in the primary splenocyte culture medium was quantified spectrophotometrically using the Griess reagent- G2930 (Promega Corp., Madison, USA). The absorbance at 540 nm was measured, and the NO concentration was determined using a calibration curve with sodium nitrite as a standard chemical.

2.10. Measurement of serum cytokine level

Level of the cytokines (IL-1 β , IL-6, TNF- α , IFN- γ , IL-12p70, and IL-10) in serum was determined using Multiplex Bead Array System (Bio-Rad, Hercules, USA). The cytokine multiplex bead array kit was purchased from Bio-Rad, San Diego, CA, USA and used according to the manufacturer's specifications. Data acquisition and analysis were carried out on 5-parameter logistic method.

3. Statistical analysis

All data are presented as the mean \pm SEM. The mean values among different groups were analyzed and compared using one-way analysis of variance (ANOVA) followed by subsequent multiple comparison test (Tukey) with Graph Prism version 5.0 software packages (Graph Pad software, La Jolla, USA). One way ANOVA with repeated measurements followed by Tukey's test was applied to test the influence of ZnO NPs on body weight gain. Statistical significance levels were defined at $p < 0.05$.

III. RESULTS

1. ZnO NP preparation

1.1. Dispersion tests

Nanoparticles (NPs) specifically, due to their high specific surface area compared to large particles, usually form agglomerates or aggregates, furthermore, they can be readily precipitated when dispersed in aqueous solution. The dispersion behaviors of ZnO NPs were examined in PBS pH 7.4, L-Serine/HEPES pH 6.2 and Citrate/HEPES pH 7.3 conditions. As shown in Figure 1, PBS pH 7.4 was not determined to be effective in dispersing ZnO NPs and required more extensive mixing. In contrast, L-Serine/HEPES pH 6.2, and Citrate/HEPES pH 7.3 exhibited higher dispersion homogeneity of ZnO NPs than PBS pH 7.4. We found that the optimum physical mixing method in our experiments is simple vortexing for 5 min, followed by the ultra-sonication with a probe sonicator for 10 sec. To prevent reagglomeration, ZnO NP stock solution was prepared just before the experiment. The working ZnO NP suspension with four different concentrations (5, 10, 20, 40 $\mu\text{g/ml}$) was prepared in cell culture media (DMEM). The turbidity of working solution was increased by the increment of ZnO NP concentration.

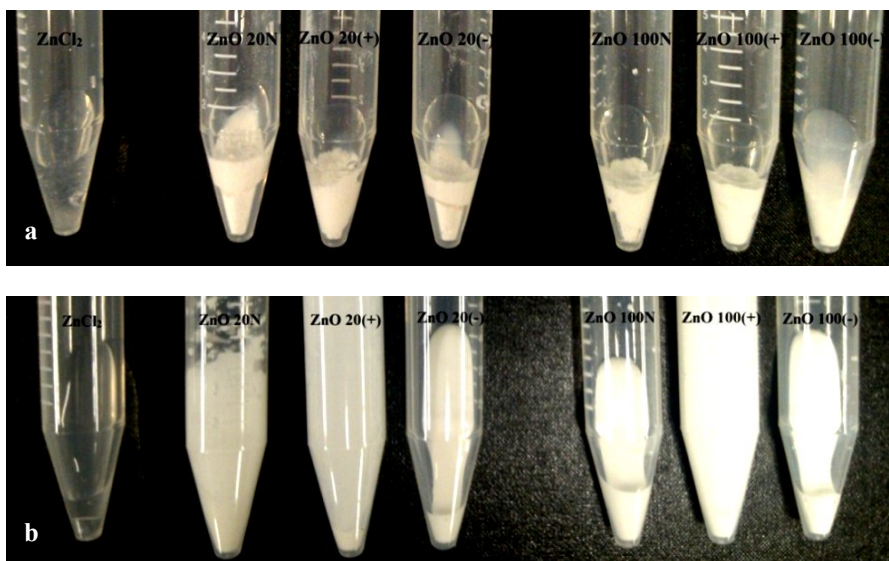


Figure 1. Digital images of ZnO NPs in three different aqueous solutions (PBS pH 7.4, L-Serine/HEPES pH 6.2, Citrate/HEPES pH 7.3), and ZnCl₂ in PBS pH 7.4 before (a) and after (b) mixing with vortex for 5 min.

1.2. Physicochemical characterizations of ZnO NPs

The pristine ZnO NPs were determined to have an average particle size of ~ 20 and ~ 70 nm, respectively, with homogeneous distribution (Fig. 2a and d). We could observe distinct grain boundaries in each SEM images which means that the present NPs do not form significant aggregates. The ZnO NPs dispersed in either Serine/HEPES pH 6.2 or Citrate/HEPES pH 7.3 also showed similar average particle size and homogeneity in distribution (Fig. 2b, c, e and f). The grain boundaries of ZnO NPs dispersed in either Serine/HEPES pH 6.2 or Citrate/HEPES pH 7.3 is rather blurred compared to that of pristine ones, which is attributed the organic moieties (serine or citrate) coated on the surface of NPs, however, we could not observe significant agglomerate formation in those NPs.

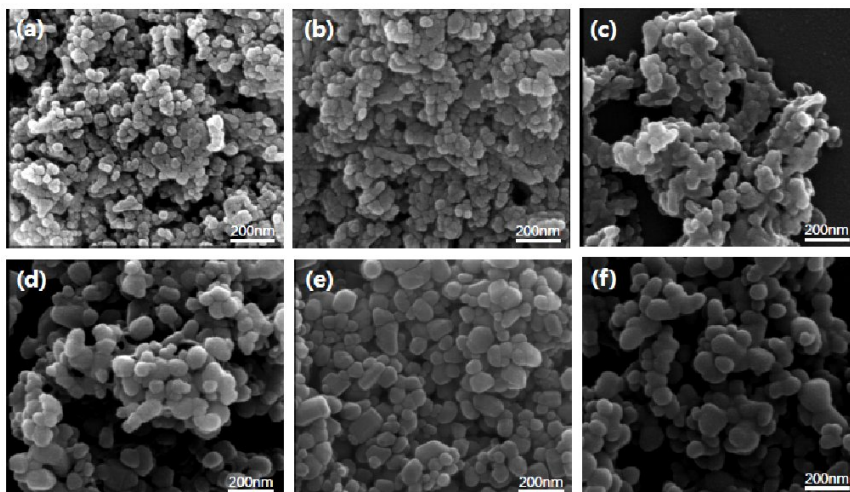


Figure 2. Scanning electron microscopic images of ZnO NPs (a) pristine ZnO²⁰ (b) ZnO²⁰ dispersed in Serine/HEPES pH 6.2 (c) ZnO²⁰ dispersed in Citrate/HEPES pH 7.3 (d) pristine ZnO⁷⁰ (e) ZnO⁷⁰ dispersed in Serine/HEPES pH 6.2 and (f) ZnO⁷⁰ dispersed in Citrate/HEPES pH 7.3.

2. *In vitro* immunotoxicity

Multitude studies suggested that ZnO NP exposure to eukaryotic cells would generate ROS in corresponding cells, thereby leading to cellular damage or even cell death. However, the influence of ZnO NP size and charge on immune cell remains unclear. To clarify this, using four type of ZnO NPs, we examined cell viability (end-point, and real time assay), the level of intracellular reactive oxygen species (ROS), mitochondrial membrane potential (MMP), and antioxidant enzyme activities such as superoxide dismutase (SOD), glutathione peroxidase (GPx) in macrophage cell line, Raw 264.7 cells.

2.1. End-point cell viability

The effect of ZnO NPs on the viability of Raw 264.7 cells was examined using CCK-8 assay (Fig. 3). ZnO NPs at the concentrations 0-5 $\mu\text{g/ml}$ had minimal effect on the viability of Raw 264.7 cells, although it significantly reduced the viability at higher concentration range (10-80 $\mu\text{g/ml}$) after 24 h incubation. To compare the potency of each ZnO NP, EC_{50} value was calculated according to sigmoidal dose-response regression (Tab. 1). ZnCl_2 was used as a positive control. Of note, ZnCl_2 was less cytotoxic than ZnO NPs ($\text{EC}_{50} = 14.34 \mu\text{g/ml}$). The range of EC_{50} of ZnO NPs was 7.591-10.37 $\mu\text{g/ml}$: ZnO 100(+) exerted the highest cytotoxicity against Raw 264.7 cells ($\text{EC}_{50} = 7.591 \mu\text{g/ml}$), while the cytotoxicity strength of other ZnO NPs was ZnO 20(+) > ZnO 100(-) > ZnO 20(-) in descending order. Additionally, EC_{50} values of positively charged ZnO NPs were higher than those of negatively charged ZnO NPs, suggesting that the size and charge of ZnO NPs could affect their cytotoxicity.

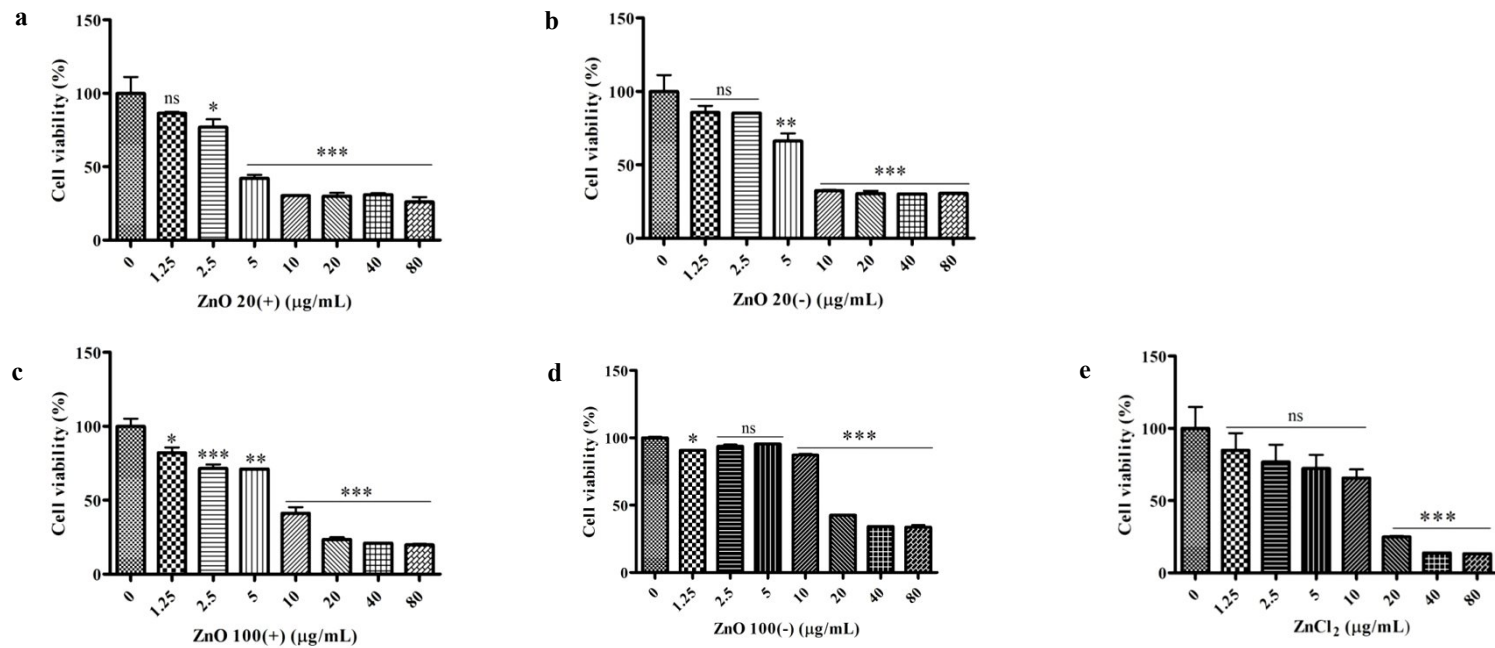


Figure 3. Effect of ZnO NPs and ZnCl₂ on the viability of Raw 264.7 cells. Cells were incubated with indicated concentrations of ZnO NPs or ZnCl₂ for 24 h (a: ZnO 20(+), b: ZnO 20(-), c: ZnO 100(+), d: ZnO 100(-), e: ZnCl₂), and DMEM media was used as a negative control. Cell viability was then determined by a CCK-8 assay. All values are presented as mean ± SEM of the three experiments conducted in duplicate. **p*<0.05, ***p*<0.001, ****p*<0.001 *versus* control cells incubated with media only.

Table 1. EC₅₀ values (24 h growth inhibition) of ZnO NPs and ZnCl₂ on Raw 264.7 cells.

	ZnO				ZnCl₂
	(+) 20 nm	(-) 20 nm	(+) 100 nm	(-) 100 nm	Neutral
EC ₅₀ (µg/ml)	8.434	10.37	7.591	8.627	14.34
95% confidence limit (µg/ml)	7.895-8.973	6.627-14.12	6.716-8.465	7.497-9.846	10.87-17.84

(+): Positive charge. (-): Negative charge. Neutral: No charge.

All values are presented as mean ± SEM of the three experiments conducted in duplicate.

2.2. Real-time cell viability

To evaluate the real-time kinetics of ZnO NPs-induced cytotoxicity, the impedance-based apparatus (xCelligence) was used to measure cell viability during 96 h (Fig. 4). In CCK-8 assay, the positive charged or the bigger sized NPs displayed remarkable toxicity in Raw 264.7 cells than the negatively charged or the smaller sized one. By contrast, real time assay showed that at the concentration of 5 $\mu\text{g}/\text{ml}$, size effect was reverse wherein ZnO (20+/-) were more cytotoxic to Raw 264.7 than ZnO (100+/-), whereas at the concentration of 20 $\mu\text{g}/\text{ml}$ size effect was not noticeable. Cytotoxicity of the same charged ZnO NPs was more intense at lower concentration than at higher one. Consistent with our data in the end point treatment, the positively charged ZnO NPs were more cytotoxic to Raw 264.7 cells than the negatively charged one. Consequently, our findings indicate that different size and charge of ZnO NPs induce differential cytotoxicity against Raw 264.7 cells, suggesting that the size and charge of ZnO NPs would affect their cytotoxicity.

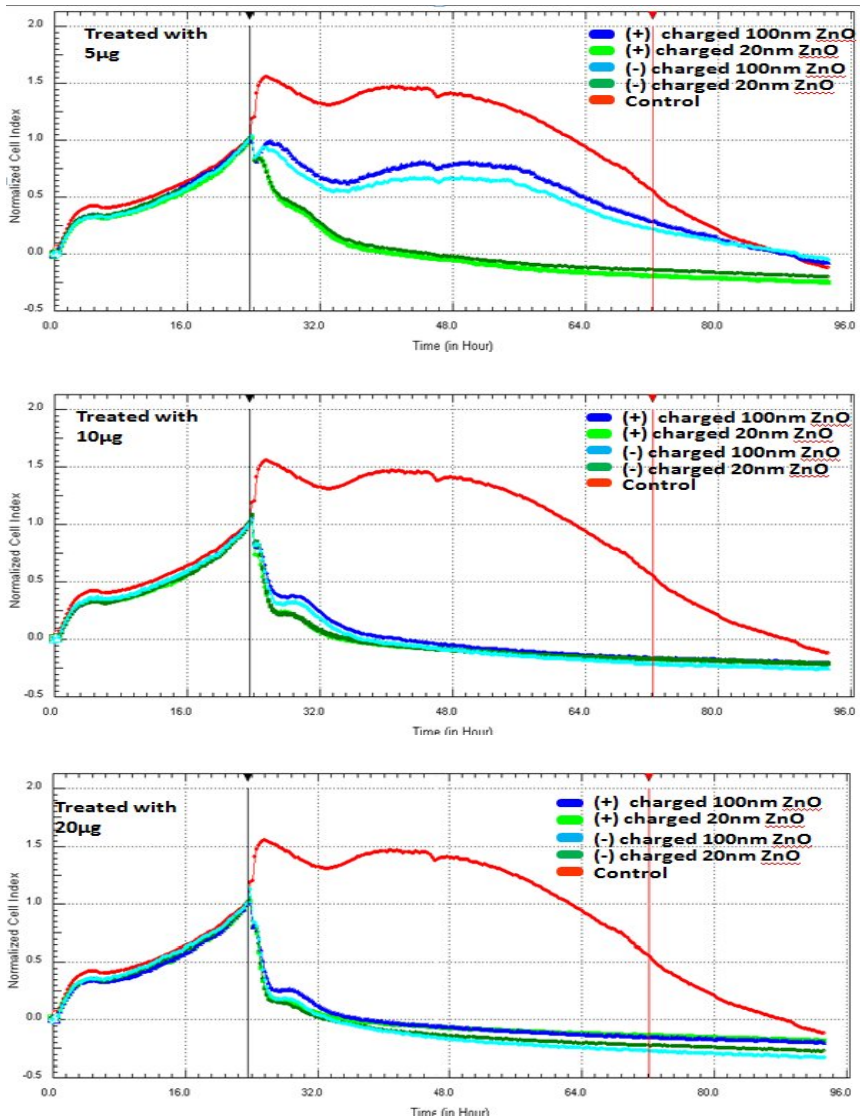


Figure 4. Effect of ZnO NPs on real-time cell viability of Raw 264.7 cells. Cells were seeded into E-plate 16 and treated with indicated concentrations of ZnO NPs. Real-time cell impedance was monitored every 15-20 min to produce time dependent cell response dynamic curves. All values are represented as mean \pm SEM of an experiment conducted in triplicate.

2.3. ZnO NPs induce the generation of intracellular ROS in Raw 264.7 cells

To investigate whether ZnO NPs could modulate ROS generation, and further elucidate the influence of NP size and charge in their toxicity, we treated ZnO NPs onto Raw 264.7 cells for the different indicated time points (0.5-1-3-6-24 h), followed by detecting DCF-DA intracellular ROS (Fig.5). We found that 20 µg/ml ZnO NPs treatment significantly increased intracellular ROS generation in a time-dependent manner: started generating intracellular ROS at 0.5 h, then peaked at 1 h except ZnO 20(+). Thereafter, the level of ROS in all ZnO NPs group decreased down to the baseline at 6 h. In terms of ROS productivity, ZnO 20(+) was most potent: ZnO 20(+) exerted the highest level of intracellular ROS generation (~2.5 fold increase) as compared to control after 0.5 h treatment. Interestingly, ROS levels of ZnO NPs at 1 h treatment were consistent with cell viability data: the bigger sized or the positively charged ZnO NPs induced higher level of intracellular ROS than the smaller sized or the negatively charged one. However, the size and charge effect of ZnO NPs on the ROS generation was unclear at other time points.

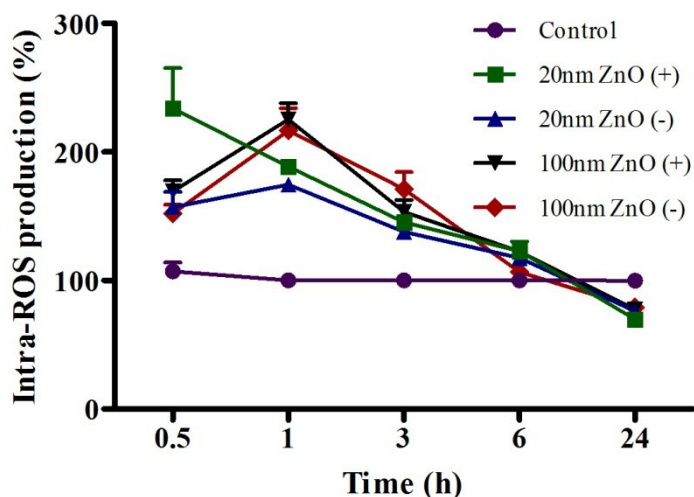


Figure 5. Effect of ZnO NPs on intracellular ROS generation in Raw 264.7 cells. Cells were incubated with four types of ZnO NPs for different indicated times (0.5-1-3-6-24 h), and DMEM media was used as a negative control. Cells were then loaded with H₂DCF-DA for 15 min, washed twice with NPSS and intracellular ROS generation was measured using DTX-880 multimode microplate reader. All values are represented as mean \pm SEM of the two experiments conducted in triplicate, and normalized with control as 100%.

2.4. Effect of ZnO NPs on mitochondrial membrane potential (MMP)

The above observations suggested that ROS generation induced by ZnO NPs might be related to cytotoxicity to Raw 264.7 cells. Next, we addressed whether ZnO NP-induced cytotoxicity would be related to mitochondrial function. Toward this, we measured the ratio of red/green fluorescence after 3 h treatment using JC-1, mitochondrial membrane potential sensor (Fig. 6). Overall, treatment with ZnO NPs except ZnO 100(-) significantly dropped the ratio of red/green fluorescence compared to control, which indicated the decrement of mitochondrial membrane potential (MMP). By contrast, no change in MMP was observed in ZnO 100(-) treated cells. Additionally, MMP of the positively charged ZnO NP-treated cells was lower than that of the negatively charged one.

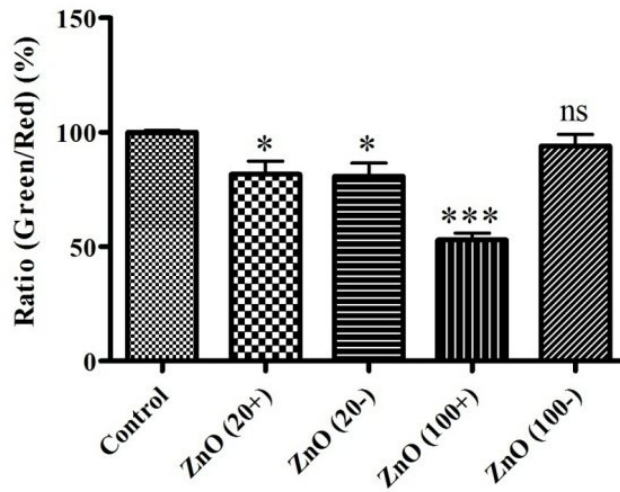


Figure 6. Effect of ZnO NPs on mitochondrial membrane potential (MMP) in Raw 264.7 cells. Cells were incubated with four types of ZnO NPs for 3 h, and DMEM media was used as a negative control. Cells were then loaded with JC-1 for 15 min, washed twice by NPSS and MMP was measured using Flex Station II384. All values are represented as mean \pm SEM of the two experiments conducted in triplicate, and normalized with control as 100%. * $p < 0.05$, *** $p < 0.001$ versus media alone.

2.5. Effect of ZnO NPs on antioxidant enzyme (SOD, GPx) activity

Superoxide dismutase (SOD) is a group of enzyme known as the first defense against oxidative stress. SOD modulates the formation of H_2O_2 from $O_2^{\cdot-}$. However, glutathione peroxidase (GPx) transforms H_2O_2 into water. Consequently, the alteration of SOD and GPx could affect ROS activity in both cytosol and mitochondria, thus leading to cell death or cell proliferation. To test whether ZnO NPs would affect anti-oxidant enzyme activity, ZnO NPs were treated onto Raw 264.7 cells for 3 h, followed by measuring the activity of SOD and GPx (Fig. 7). We found that SOD activity was reduced when treated with the positively charged ZnO NPs (Fig. 7a). Meanwhile, there is no significant size effect of ZnO NP on SOD activity. SOD activity was reduced by the positive charged ZnO NPs only, albeit barely affected by the negative charged ZnO NP treatment. Next, GPx activity was examined. Overall, all ZnO NPs treatment decreased GPx activities in Raw 264.7 cells (Fig. 7b). However, the positive charged ZnO NPs further decreased GPx activity in Raw 264.7 cells than the negative charged one. Taken together, the charge effect is more prominent in GPx activity than in SOD activity. Importantly, in terms of enzyme activities, the activity of GPx is more correlated to the ROS level rather than SOD.

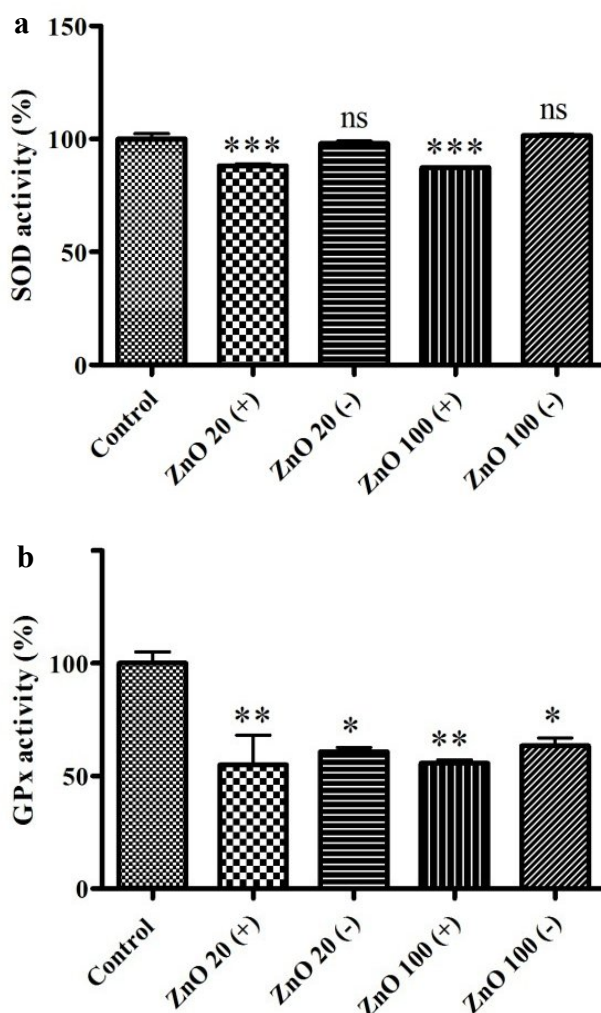


Figure 7. Effect of ZnO NPs on (a) superoxide dismutase (SOD), and (b) glutathione peroxidase (GPx) activity in Raw 264.7 cells. Cells were incubated with four types of ZnO NPs for 3 h, and DMEM media was used as a negative control. Cells were then collected and assayed as manufacture's instruction. All values are represented as mean \pm SEM of the two experiments conducted in triplicate, and normalized with control as 100%. * p <0.05, ** p <0.01, *** p <0.001 *versus* media alone.

3. *In vivo* immunotoxicity

3.1. Change of body weight and behavior

To assess the immunotoxicity *in vivo*, C57BL/6 mice were orally administered with ZnO NPs every day continuously for 14 days. The change of relative mouse body weight gain with time was shown in Figure 8. The positive ZnO NP-fed mice experienced a slight weight loss (all less than 10% of body weight on the day 0) on the day 5 and 10, then it was recovered on the day 14. Specifically, compared to control, the body weight gain of ZnO 20(+)-, and ZnO 100(+)-fed mice are significant lower at the day 5, 10, and 14 post treatment. By contrast, the negative ZnO NPs did not significantly induce body weight loss in mice. Nevertheless, none of mice died, and they did not show any alteration in behavior during the treatment period.

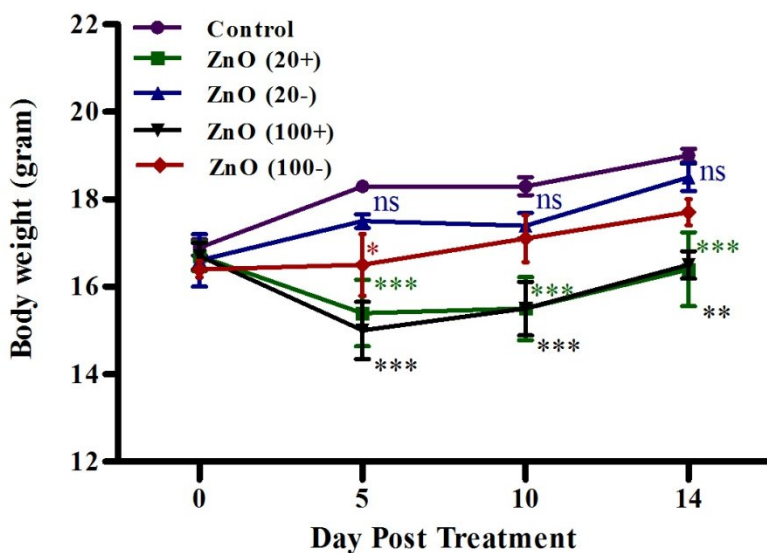


Figure 8. Body weight change of mice after ZnO NP administration. Body weight was measured on days 0, 5, 10 and 14 after administration of ZnO NPs. Day 0 was designated as the day of administration. Values are presented as mean \pm SEM, $n=5$. * $p<0.05$, ** $p<0.01$, *** $p<0.001$ versus control.

3.2. Spleen weight, and coefficient of spleen to body weight

After 14 day ZnO NP oral administration, mice were sacrificed, spleens were collected and weighed. Spleen weight and the coefficient of spleen to body weight were shown in Figure 9. No significant differences of spleen weights were noted (Fig. 9a). However, in ZnO 20(+)-fed mice, the coefficients of spleen to body weight was significantly higher than control (Fig. 9b). This was consistent with the body weight loss induced by ZnO 20(+) as shown in Figure 8.

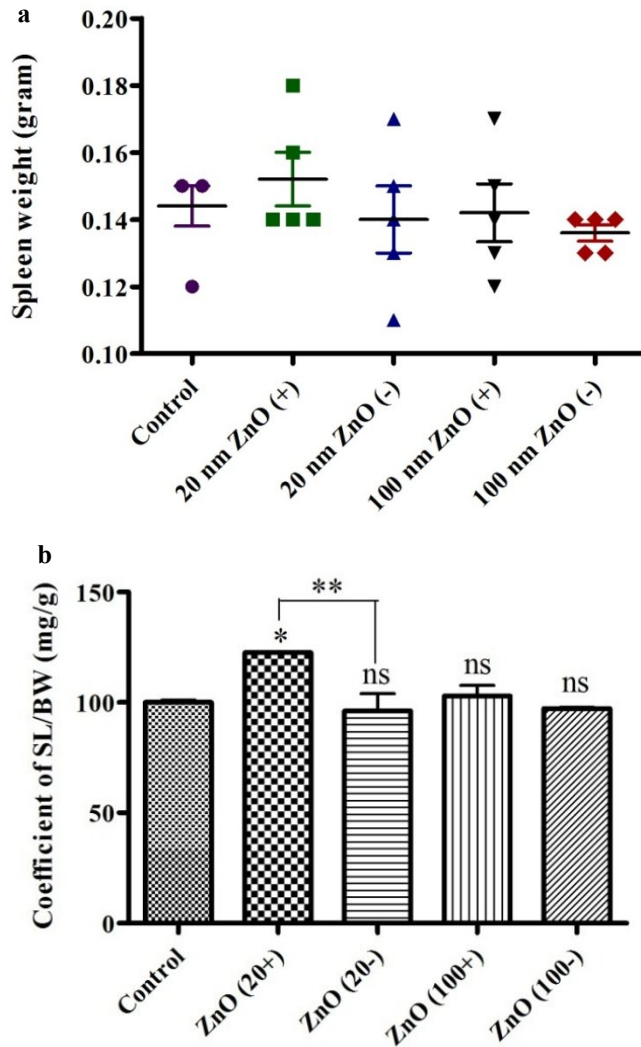


Figure 9. Effects of ZnO NPs on spleen weight (a), and coefficient of spleen to body weight (b) after 14 day ZnO NP oral administration. Spleen was weighed, and coefficient of spleen to body weight was calculated and normalized with control as 100%. Values are presented as mean \pm SEM, $n=5$. * $p<0.05$, ** $p<0.01$ versus control.

3.3. Immunotoxicity parameters

3.3.1. Immunophenotyping

ZnO NP treatment slightly induced the alteration in cell distribution of splenocytes (Fig. 10, Tab. 2). While T helper (CD^{4+}) and T cytotoxic (CD^{8+}) cells accounted for 16.6% and 9.1%, respectively of the control, the distribution of T helper and T cytotoxic cells in splenocytes of treated groups (ZnO 20 (+/-), ZnO 100 (+/-)) was changed to 14.66/9.18%, 15.44/11.62%, 14.53/10.22%, 16.80/11.60%, respectively. Notably, the percentage of T helper cells was significantly reduced when treated with ZnO 100(+) as compared to control (Fig. 10a, Tab. 2). Moreover, the ratio of CD^{4+} T cells to CD^{8+} T cells, which are subpopulations of T cells (T helper cells and T cytotoxic cells), significantly changed from 1.634 fold to 1.301 fold in ZnO 100(+)-fed mice. However, little differences were noted in the proportion of B cell, NK cell, and monocyte subpopulations.

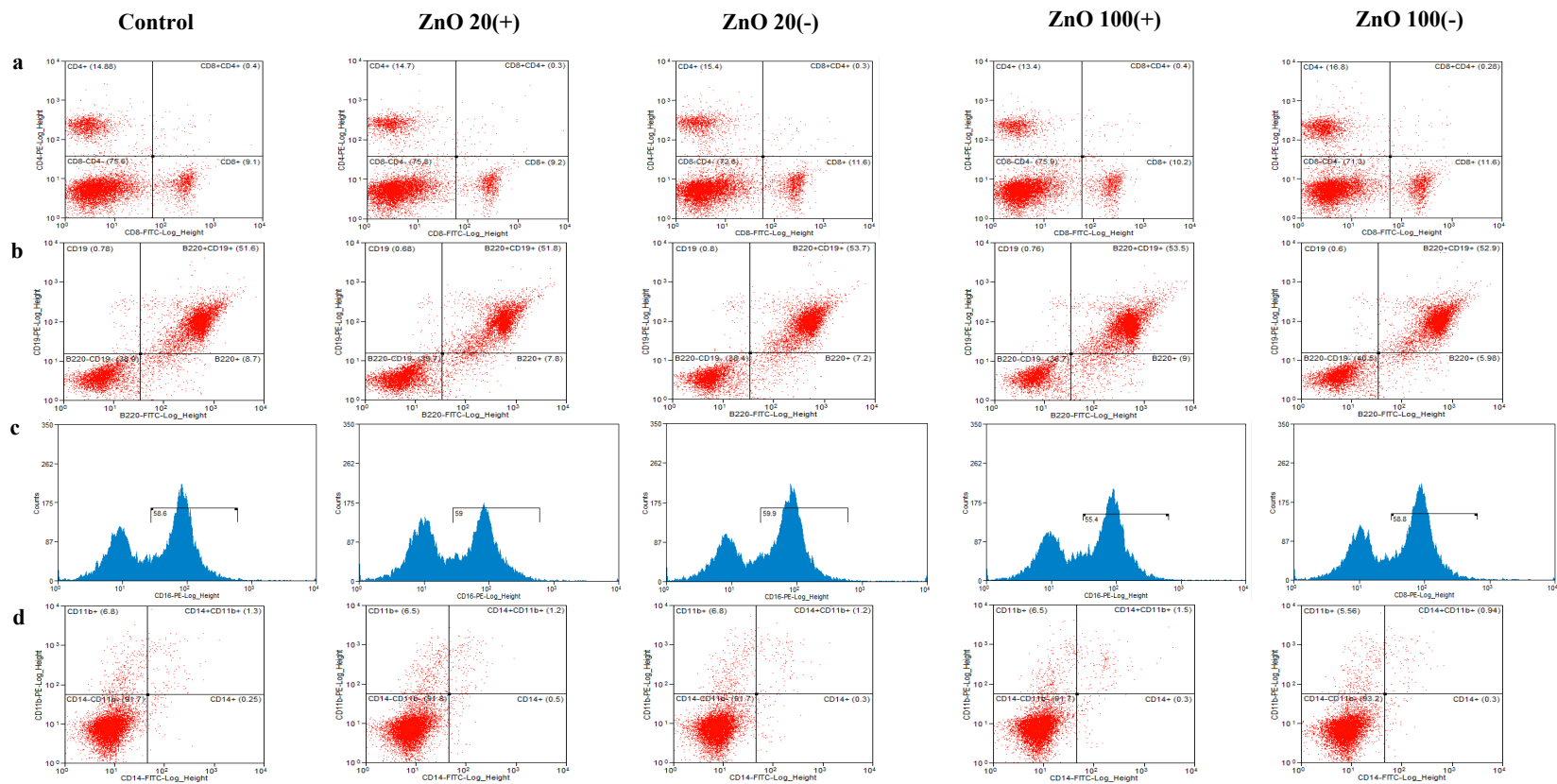


Figure 10. Distribution of leukocytes from spleen after ZnO NPs oral administration for 14 days. Splenocytes were isolated, then the cell mixture was stained with fluorescently labeled CD4, CD8, CD19, B220, CD16, CD14, CD11 antibodies to identify subpopulations, washed to remove excess antibody and analyzed by flow-cytometry. Data were obtained by gating on 10,000 events, (a) T cell subpopulation, (b) B cell subpopulation, (c) NK cell subpopulation, (d) Monocyte subpopulation distribution in the splenocytes.

Table 2. Immunophenotype of splenocytes in C57BL/6 mice administered with ZnO NPs for 14 days

Administration	PBS	ZnO 20(+)	ZnO 20(-)	ZnO 100(+)	ZnO 100(-)
^a CD4 ⁺ CD8 ⁻	16.60 ± 0.60	14.66 ± 0.80	15.44 ± 0.54	14.53 ± 1.37*	16.80 ± 0.69
^b CD4 ⁺ CD8 ⁺	9.10 ± 1.18	9.18 ± 0.42	11.62 ± 0.53	10.22 ± 0.64	11.60 ± 0.33
CD4 ⁺ CD8 ⁺	0.4 ± 0.04	0.32 ± 0.04	0.32 ± 0.04	0.38 ± 0.11	0.28 ± 0.05
B220 ⁺ CD19 ⁻	0.78 ± 0.09	0.68 ± 0.04	0.80 ± 0.07	0.83 ± 0.09	0.60 ± 0.03
B220 ⁻ CD19 ⁺	8.70 ± 1.09	7.82 ± 0.38	7.20 ± 0.42	9.02 ± 1.32	5.98 ± 2.23
^c B220 ⁺ CD19 ⁺	51.58 ± 1.56	51.78 ± 2.52	53.70 ± 0.54	53.50 ± 0.55	52.92 ± 1.04
^d CD16 ⁺	58.55 ± 1.30	59.02 ± 2.26	59.88 ± 0.53	55.44 ± 6.69	58.76 ± 1.17
CD11 ⁺ CD14 ⁻	6.80 ± 0.27	6.54 ± 0.22	6.80 ± 0.34	6.52 ± 0.71	5.56 ± 0.23
CD11 ⁻ CD14 ⁺	0.25 ± 0.03	0.42 ± 0.06	0.26 ± 0.06	0.30 ± 0.03	0.30 ± 0.04
^e CD11 ⁺ CD14 ⁺	1.23 ± 0.06	1.04 ± 0.07	1.04 ± 0.12	1.50 ± 0.21	0.94 ± 0.07
CD4 ⁺ /CD8 ⁺	1.643 ± 0.07652	1.599 ± 0.06671	1.338 ± 0.06395	1.301 ± 0.07723*	1.450 ± 0.05374

Values are presented as mean ± SEM, *n*=5; **p*<0.05; a: T helper cells, b: T cytotoxic cells, c: B cells, d: Macrophages, e: Monocytes.

3.3.2. Innate, cell-mediated immune response (DTH and mitogenic response) against ZnO NPs

To assess the effect of ZnO NPs on regulation of innate immune response, NK cell activity was examined using NK-sensitive YAC-1 target cells. As shown in Table 3, a decrease of NK cell activity was observed in the mice treated with ZnO NPs. At the ratio of 100:1, ZnO NPs significantly inhibited NK cell activity.

Next, we examined the effect of ZnO NPs on cell-mediated immunity using DTH response on C57BL/6 mice. The swelling volume is similar after 24 h and 48 h challenge (Tab. 4). An increased DTH response to ZnO NPs was observed. However these differences were not statistically significant. Further, we analyzed the mitogen-stimulated proliferative responses of T and B lymphocytes (Fig. 12). These responses were elevated compared to control but not significant. Taken together, ZnO NPs affected NK activity but not cell mediated immunity.

Table 3. NK cell activity in ZnO NP-fed mice.

Effector/Target Ratio	NK cell activity (%; Mean \pm SEM)				
	Control	ZnO 20(+)	ZnO 20(-)	ZnO 100(+)	ZnO 100(-)
100:1	10.245 \pm 0.698	0 ***	3.335 \pm 2.061 ***	0 ***	0 ***
50:1	4.037 \pm 0.591	0 *	0.105 \pm 0.061 *	1.415 \pm 0.930	1.655 \pm 1.655
25:1	1.923 \pm 1.589	0	0.502 \pm 0.435	0	1.263 \pm 1.263

YAC-1 cells were used as a target; and effector cells (NK cells) were isolated from the spleen of mice fed with sublethal dose of ZnO NPs for 14 days. ZnO NP treatment reduced NK cell cytotoxicity in the treated groups compared to control. Values are presented as mean \pm SEM of percent (%) cytotoxicity, $n=5$. * $p<0.01$, *** $p<0.001$.

Table 4. Delayed type hypersensitivity in ZnO NP-primed mice.

Treatment	Foot-pad swelling (mm)			
	24 h		48 h	
	Saline	ZnO NP	Saline	ZnO NP
ZnO 20(+)	6.780 ± 1.484	7.242 ± 1.318	6.823 ± 0.3485	7.812 ± 0.7510
ZnO 20(-)	1.523 ± 0.9862	1.202 ± 1.103	1.557 ± 0.3313	1.706 ± 0.5497
ZnO 100(+)	10.55 ± 0.4293	11.70 ± 2.053	7.140 ± 0.6409	10.48 ± 1.521
ZnO 100(-)	4.317 ± 0.8631	4.718 ± 1.730	1.340 ± 0.7702	1.338 ± 0.6657

Measurement of footpad swelling in mice induced by DTH response after 24 h and 48 h challenge. Values are presented as mean ± SEM, *n*=5.

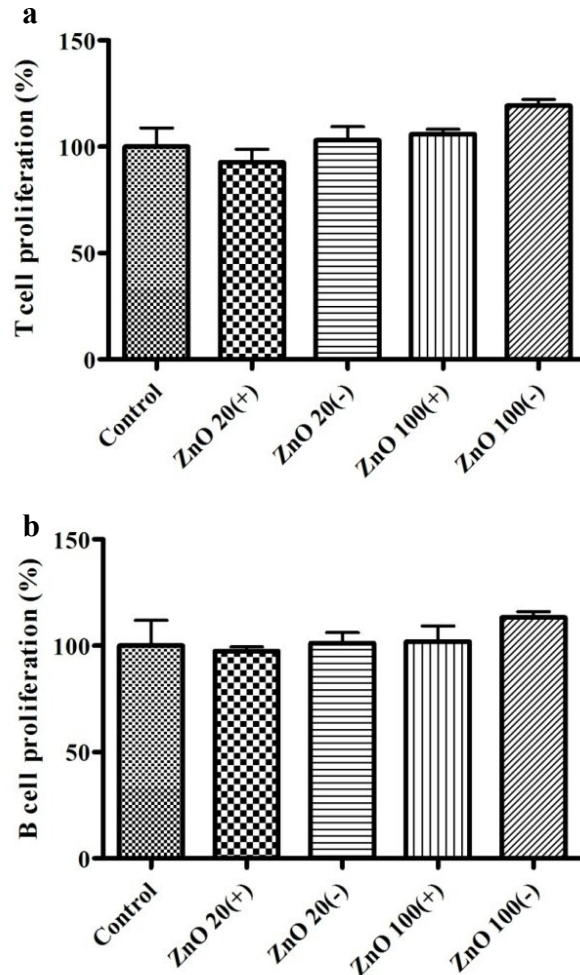


Figure 11. Mitogenic response of mouse splenocytes. Splenocytes (2×10^6 cells/ml) were incubated for 24 h with concanavalin A (Con A) , or lipopolysacchride (LPS) to evaluate T lymphocyte (a) and B lymphocyte (b) proliferation, respectively. Values are presented as mean \pm SEM, and normalized with control as 100%.

3.3.3. NO production of splenocytes

NO is a reactive nitrogen which is an important cellular signaling molecule involved in several biological processes, moreover serves as one of the key mediator of immune defenses. To further explore the impact of ZnO NPs on immune defense, we measured the level of splenic NO production after 14 day treatment. As shown in Figure 12, a significant decrease in NO level occurred after administration of ZnO 20(-), and ZnO 100(+/-). However, there was no substantial difference of NO level in ZnO 20(+)-fed mice as compared to the control.

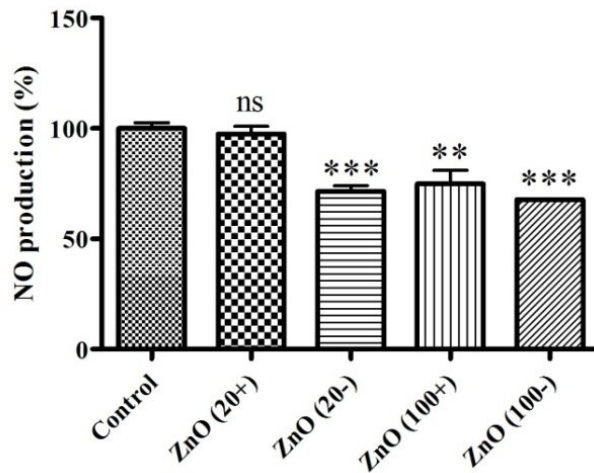


Figure 12. Nitric oxide (NO) production induced by ZnO NPs in mouse splenocytes. Splenocytes were isolated and cultured. The culture supernatant was then used to measure nitric oxide (NO) production using Griess reagent. Values are presented as mean \pm SEM, and normalized with control as 100%. $n = 5$. ** $p < 0.01$, *** $p < 0.001$.

3.3.4. Serum cytokine level

To explore immune status change induced by ZnO NPs we examined serum pro- and anti-inflammatory cytokine (IL-1 β , IL-6, TNF- α , IL-12p70, IFN- γ , and IL-10) level at the end point treatment. We found that overall the level of serum cytokines in ZnO-fed mice were lower than saline-fed mice (Fig. 13). In particular, serum levels of pro-inflammatory cytokines (IL-1 β , TNF- α , and IL-12p70) in ZnO NP-fed mice were ZnO 20(+) > ZnO 20(-) > ZnO 100(+) > ZnO 100(-) in descending order. Accordingly, the level of IL-10, an anti-inflammatory cytokine in ZnO NP-fed mice tended to be significantly lower than PBS-fed mice. By contrast, there was no significant change of cytokine level in ZnO 20(+)-fed mice. In terms of size and charge effect on serum cytokine level, the size and charge were correlated to serum cytokine level. Further, the size appears more correlated to the serum cytokine than the charge. Taken together, our data show that oral intake of ZnO NPs in mice could drop the level of serum cytokines, importantly implying the possible suppression of immune status of C57BL/6 mice fed with ZnO NPs.

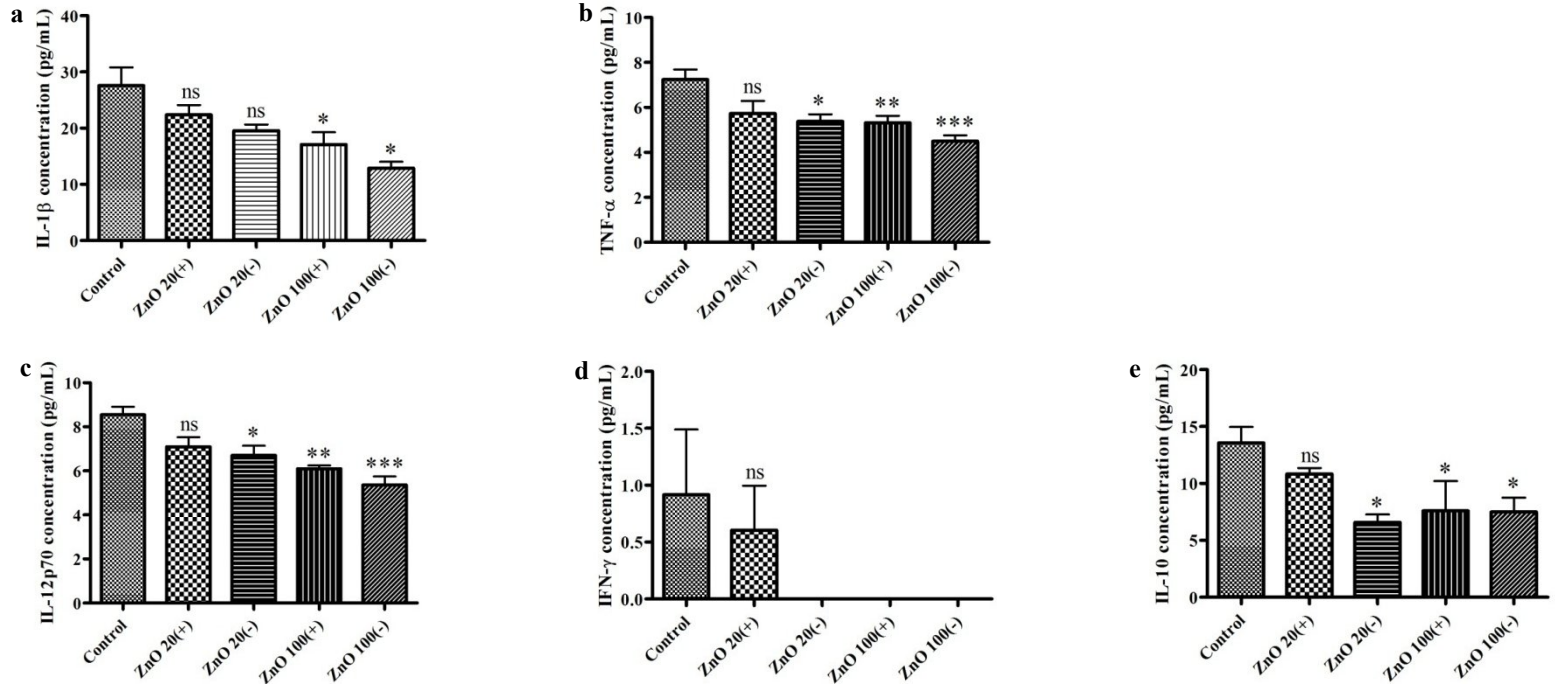


Figure 13. Serum cytokine profiles in ZnO NP-fed mice. After 14 day administration, mice were retro-orbital bled, isolated serum by centrifugation and the level of IL-1 β (a), TNF- α (b), IL-12p70 (c), IFN- γ (d), and IL-10 (e) were examined using Multiplex Bead Array System (Bio-Rad). IL-6 is lower than detectable limitation. Values are presented as mean \pm SEM, $n=5$. * $p<0.05$, ** $p<0.01$, *** $p<0.001$.

IV. DISCUSSION

Convincing evidences showed that ZnO NPs would have a potential to deliver to several organ such as liver, spleen, kidneys, brain or heart after exposure (Yeh et al. 2012, 085102). In this regard, ZnO NPs accessed in human body would interact with immune cell, thus, damaging immune tissues and organs. However, the immunotoxicity of ZnO NPs in relation to specifically the size and charge of ZnO NP are unclear. To address this issue, we assessed the immunotoxicity of ZnO NPs *in vitro* and *in vivo* and explored their underlying mechanism. First, *in vitro* study indicates that ZnO NPs induce cytotoxicity to immunocytes via ROS generation, which is influenced by the size and charge of ZnO NPs. To validate this, we examined cell viability using colorimetric (CCK-8 assay) and impedance assay (real-time kinetic assay), intracellular ROS production, mitochondria membrane potential (MMP), and antioxidant enzyme activity (SOD, GPx) in Raw 264.7, macrophage cell line.

Cell viability assays (CCK-8, real-time xCelligence) showed that ZnO NPs with different sizes and charges have differential cytotoxicity to Raw 264.7 cells (Fig. 3). Interestingly, the positively charged NPs exerted higher cytotoxicity against Raw 264.7 cells than the negatively charged one. On the contrary to static CCK-8 assay, real-time dynamic assay revealed that ZnO NPs at the concentration of 5 $\mu\text{g/ml}$ displayed differential cytotoxicity pattern, albeit similar at higher concentrations (10-20 $\mu\text{g/ml}$) (Fig. 4). ZnO NP-induced cytotoxicity could be affected by the release of Zn^{2+} ions through the dissolution of ZnO NPs within aqueous culture media (Cho et al. 2011, 27, George et al. 2010, 15-29, Xia et al. 2008, 2121-34). Hence, a control experiment was performed with ZnCl_2 . In term of EC_{50} , we found that ZnO NPs would cause

cytotoxicity at lower dose compared to ZnCl₂ (Tab. 1). This difference might be due to inherent features of metal oxides: free Zn²⁺ ions, and oxidative radical-generated oxide, and ZnO NP surface charge would synergistically exert cytotoxicity to eukaryotic cells.

Next, we checked ROS production to uncover the mechanism of ZnO NP-induced cytotoxicity. ZnO NPs have been shown to generate the formation of ROS (Song et al. 2010, 389-97, Xia et al. 2008, 2121-34), which is the major molecule to exert the cytotoxicity to biologic cells. Since ZnO NPs were dispersed in aqueous solution, their active sites could interact with water or oxygen to generate ROS, such as superoxide anions, hydroxyl radicals, and singlet oxygen, thereby resulting in cell stress or even cell death. In that context, we hypothesized that ZnO NPs would induce cell stress by way of generating ROS. For this, intracellular ROS production was examined at the indicated time points (0.5-1-3-6-24 h). We found that the intracellular ROS production induced by ZnO NPs is time-dependent (Fig. 5). For instance, ZnO NPs at higher concentration induced higher level of intracellular ROS at short treatment time (< 6 h), albeit almost same levels to control after 6 h. Long time (> 6 h) incubation would increase the reagglomeration of ZnO NPs, eventually, decreasing cytotoxicity. Importantly, we found that the positively charged ZnO NPs exhibited higher level of intracellular ROS generation than the negatively charged one.

Since the production of ROS has been shown to disrupt the MMP enough to induce apoptosis (Curtin, Donovan, and Cotter 2002, 49-72, Orrenius, Gogvadze, and Zhivotovsky 2007, 143-83), we assessed the impact of ZnO NPs on the MMP (Fig. 6). Following exposure to the negative charge 100 nm ZnO,

there was no change in the MMP when compared to control cells. By contrast, a significant alteration in the MMP was observed following exposure to the ZnO 20(+/-) and ZnO 100(+). There is no correlation between the production of ROS elicited by all four types of ZnO NPs and their MMP patterns. This discrepancy might be ascribed to unique cell death mechanism of every ZnO NPs irrespective of the size and charge. For instance, since ZnO NPs might accumulate outside the mitochondria, their surface charges would affect the charge on the outer portion of the mitochondrial membrane, leading to an imbalance in the MMP.

Last, to assess oxidative stress parameters we examined the antioxidant enzyme activities (SOD, GPx) induced by ZnO NPs (Fig. 8). Overall, all ZnO NPs treatment decreased both SOD and GPx activities of Raw 264.7 cells. SOD is a defense enzyme against the harmful effect of ROS, which converts $O_2^{\cdot-}$ into H_2O_2 , thereafter H_2O_2 can be degraded into H_2O by GPx (Valko et al. 2007, 44-84). The generation of ROS, specifically $O_2^{\cdot-}$ can damage mitochondrial, thus resulting in mitochondrial dysfunction (Kirkinezos, and Moraes 2001, 449-57). This decreased enzymes (SOD, GPx) activities might be owing to the generation of ROS in cells induced by ZnO NPs. Of note, in terms of enzyme activity, the activity of GPx is more correlated to the ROS level rather than SOD.

In this experiment, another merit is the validity of *in vitro* immunotoxicity test using Raw 264.7 cell line. While, this cell line is well-known standard cell line for *in vitro* immunotoxicity test, *in vitro* immunotoxicity test for nanoparticle is not established. Using this cell line, we verified the potential value of *in vitro* immunotoxicity battery for unknown nanoparticle, since the *in vitro* data might be compatible to *in vivo* immunotoxicity profiles. Collectively, our *in vitro* data clearly indicates that

different sized- and charged-ZnO NPs induce differential cytotoxicity against Raw 264.7 cells via ROS generation, MMP reduction, and anti-oxidant activity decrement. Further, we confirmed that the size and charge of ZnO NPs could affect their cytotoxicity.

Since, *in vitro* culture cannot reflect the complexity of an *in vivo* system, which is preferred for the toxicological evaluation; next, we examined the immunotoxicologic parameters induced by oral intake of ZnO NPs in mice. Our *in vivo* study indicates that the different sized- and charged-ZnO NPs could cause immunotoxicity in ZnO NP-fed mice, of which nature is a minor immunosuppression. This stems from our immunotoxicological data. Prior to immunotoxicological evaluation, we checked the weight-related parameters (body weight, spleen weight, and coefficient of spleen to body weight). Of these, only the reduced body weight gain was noted, suggesting the potential ZnO NP immunotoxicity *in vivo*. Since *in vitro* data showed ZnO-induced toxicity in immunocytes, body weight change coupled with *in vitro* data might be considered for predicting potential immunotoxicity of nanoparticles.

Next, to explore the effect of ZnO NPs on the cellular mediated immunity(CMI), we measured the delayed-type hypersensitivity (DTH) reaction to ZnO NPs, splenocyte proliferation in response to Con A and LPS, NK cell activity, and splenocyte phenotyping. Overall, no significant change was observed in DTH responses (Tab. 4), T and B cell proliferation (Fig. 11). By contrast, we found the slight change in splenocyte phenotypes (Fig. 10, Tab. 2). Since CD⁴⁺ cells can help the proliferation and differentiation of other T and B cells, and CD⁸⁺ cells can exert cytotoxicity, and regulate CD⁴⁺ cells, the ratio of CD⁴⁺/CD⁸⁺ can reflect the overall immune status in host. Of note, there was the

decreased percentage of CD⁴⁺ T cell subpopulation in ZnO 100(+)-fed mice as compared to control mice (Fig. 10a). Consistently, the ratio of CD⁴⁺/CD⁸⁺ was reduced, which might imply systemic immune suppression. These CMI variables do not tell specific function of innate arm in CMI. Toward this, we checked NK activity. Astonishingly, NK cell activity at the ratio of 100:1 was significantly decreased in all ZnO NP-fed mice compared to control (Tab. 3). NK cells were defined as lymphocytes mediating cytotoxicity against certain tumors and virus-infected target cells. In this point, the suppression of NK cell activity may reveal the weakened innate defense in CMI, consequently getting vulnerable to opportunistic dangers such as infection, cancer, and stress. Given this, we hypothesized that if these data would be valid, humoral immune mediators should be co-regulated toward the immune suppression. To verify this, we selected two humoral immune parameters (nitric oxide, cytokines).

First, we checked NO production from splenocytes of ZnO NP-fed mice. Nitric oxide (NO) is a reactive nitrogen species which plays an important role in destruction and suppression of many intracellular pathogenic organisms (Green et al. 1994, 87-94, Guzik, Korbut, and Adamek-Guzik 2003, 469-87). NO act as an effector molecule in macrophage-mediated cytotoxicity (Holan et al. 2002, 989-95). However the NO production of macrophage was regulated and required to be optimized by CD⁴⁺ T cells. We found that three oral intake of ZnO NPs except ZnO 20(+) significantly decreased NO production of splenocytes (Fig. 12). Viewed together, this is in line with the suppression of NK activity and the ratio of CD⁴⁺/CD⁸⁺ observed.

Since, NO could contribute to the regulation of immune reaction by modifying the release of cytokines (Marcinkiewicz, and Chain 1993, 146-50,

Schwentker et al. 2002, 1-10, Tavares Murta et al. 1999, 87-92), finally we quantified the serum cytokine release in ZnO-fed mice. To further analyze the several facets of *in vivo* immunotoxicity in ZnO NP-fed mice, we selected six kinds of pro- and anti-inflammatory cytokines (IL-1 β , IL-6, TNF- α , IL-12p70, IFN- γ , and IL-10). Cytokine assay showed that overall the level of serum cytokines in ZnO-fed mice were decreased as compared to control (Fig. 13). Of these cytokines, in light of the concentration serum, IL-1 β , and IL-10 were prominent in detecting the cytokine change in ZnO NP-fed mice. These cytokines were the representative pro- and anti-inflammatory cytokine, respectively. The decreased level of these opposite cytokines in ZnO NP-fed mice might be ascribed to nonspecific immune suppression or even imbalance between pro- and anti-inflammatory cytokine network. The limitation in this study is the lack of different dose usage *in vivo*. To gauge this phenomena in detail, further work will be needed.

Synthesizing these immunotoxicological data *in vivo* and *in vitro*, our results indicate that different sized- and charged-ZnO NPs would cause *in vitro* and *in vivo* immunotoxicity, of which nature is a minor immunosuppression. This has important implications for individuals who may be chronically exposed to ZnO NPs. Further, this study offered the possibility of the new immune parameters such as cytokine and NO for gauging immunotoxicity for nanoparticles.

V. REFERENCES

Cho, W. S., R. Duffin, S. E. Howie, C. J. Scotton, W. A. Wallace, W. Macnee, M. Bradley, I. L. Megson and K. Donaldson. 2011. "Progressive severe lung injury by zinc oxide nanoparticles; the role of Zn²⁺ dissolution inside lysosomes". *Particle and Fibre Toxicology*, 8: 27.

Curtin, J. F., M. Donovan and T. G. Cotter. 2002. "Regulation and measurement of oxidative stress in apoptosis". *J Immunol Methods*, 265(1-2): 49-72.

De Jong, W. H. and P. J. Borm. 2008. "Drug delivery and nanoparticles: applications and hazards". *Int J Nanomedicine*, 3(2): 133-49.

Di Gioacchino, M., C. Petrarca, F. Lazzarin, L. Di Giampaolo, E. Sabbioni, P. Boscolo, R. Mariani-Costantini and G. Bernardini. 2011. "Immunotoxicity of nanoparticles". *Int J Immunopathol Pharmacol*, 24(1 Suppl): 65S-71S.

Duguet, E., S. Vasseur, S. Mornet and J. M. Devoisselle. 2006. "Magnetic nanoparticles and their applications in medicine". *Nanomedicine (Lond)*, 1(2): 157-68.

George, S., S. Pokhrel, T. Xia, B. Gilbert, Z. Ji, M. Schowalter, A. Rosenauer, R. Damoiseaux, K. A. Bradley, L. Madler and A. E. Nel. 2010. "Use of a rapid cytotoxicity screening approach to engineer a safer zinc oxide nanoparticle through iron doping". *ACS Nano*, 4(1): 15-29.

Green, S. J., L. F. Scheller, M. A. Marletta, M. C. Seguin, F. W. Klotz, M. Slayter, B. J. Nelson and C. A. Nacy. 1994. "Nitric oxide: cytokine-regulation of nitric oxide in host resistance to intracellular pathogens". *Immunol Lett*, 43(1-2): 87-94.

Guzik, T. J., R. Korbut and T. Adamek-Guzik. 2003. "Nitric oxide and superoxide in inflammation and immune regulation". *J Physiol Pharmacol*, 54(4): 469-87.

Hanley, C., J. Layne, A. Punnoose, K. M. Reddy, I. Coombs, A. Coombs, K. Feris and D. Wingett. 2008. "Preferential killing of cancer cells and activated human T cells using ZnO nanoparticles". *Nanotechnology*, 19(29): 295103.

Hanley, C., A. Thurber, C. Hanna, A. Punnoose, J. Zhang and D. G. Wingett. 2009. "The Influences of Cell Type and ZnO Nanoparticle Size on Immune Cell Cytotoxicity and Cytokine Induction". *Nanoscale Research Letters*, 4(12): 1409-20.

Hanley, C., A. Thurber, C. Hanna, A. Punnoose, J. H. Zhang and D. G. Wingett. 2009. "The Influences of Cell Type and ZnO Nanoparticle Size on Immune Cell Cytotoxicity and Cytokine Induction". *Nanoscale Research Letters*, 4(12): 1409-1420.

Heng, B. C., X. Zhao, E. C. Tan, N. Khamis, A. Assodani, S. Xiong, C. Ruedl, K. W. Ng and J. S. Loo. 2011. "Evaluation of the cytotoxic and inflammatory potential of differentially shaped zinc oxide nanoparticles". *Arch Toxicol*, 85(12): 1517-28.

Heng, B. C., X. Zhao, S. Xiong, K. W. Ng, F. Y. Boey and J. S. Loo. 2010. "Toxicity of zinc oxide (ZnO) nanoparticles on human bronchial epithelial cells (BEAS-2B) is accentuated by oxidative stress". *Food Chem Toxicol*, 48(6): 1762-6.

Holan, V., M. Krulova, A. Zajicova and J. Pindjakova. 2002. "Nitric oxide as a regulatory and effector molecule in the immune system". *Mol Immunol*, 38(12-13): 989-95.

- Hooper, H. L., K. Jurkschat, A. J. Morgan, J. Bailey, A. J. Lawlor, D. J. Spurgeon and C. Svendsen. 2011. "Comparative chronic toxicity of nanoparticulate and ionic zinc to the earthworm *Eisenia veneta* in a soil matrix". *Environ Int*, 37(6): 1111-7.
- Jang, J., D. H. Lim and I. H. Choi. 2010. "The impact of nanomaterials in immune system". *Immune Netw*, 10(3): 85-91.
- Kirkinezos, I. G. and C. T. Moraes. 2001. "Reactive oxygen species and mitochondrial diseases". *Semin Cell Dev Biol*, 12(6): 449-57.
- Lipovsky, A., Y. Nitzan, A. Gedanken and R. Lubart. 2011. "Antifungal activity of ZnO nanoparticles--the role of ROS mediated cell injury". *Nanotechnology*, 22(10): 105101.
- Liu, Y., F. Jiao, Y. Qiu, W. Li, F. Lao, G. Q. Zhou, B. Y. Sun, G. M. Xing, J. Q. Dong, Y. L. Zhao, Z. F. Chai and C. Y. Chen. 2009. "The effect of Gd@C-82(OH)(22) nanoparticles on the release of Th1/Th2 cytokines and induction of TNF-alpha mediated cellular immunity". *Biomaterials*, 30(23-24): 3934-3945.
- Marcinkiewicz, J. and B. M. Chain. 1993. "Differential regulation of cytokine production by nitric oxide". *Immunology*, 80(1): 146-50.
- Matsumura, M., N. Takasu, M. Nagata, K. Nakamura, M. Kawai and S. Yoshino. 2010. "Effect of ultrafine zinc oxide (ZnO) nanoparticles on induction of oral tolerance in mice". *J Immunotoxicol*, 7(3): 232-7.
- Moos, P. J., K. Chung, D. Woessner, M. Honegger, N. S. Cutler and J. M. Veranth. 2010. "ZnO particulate matter requires cell contact for toxicity in human colon cancer cells". *Chem Res Toxicol*, 23(4): 733-9.
- Orrenius, S., V. Gogvadze and B. Zhivotovsky. 2007. "Mitochondrial oxidative stress: implications for cell death". *Annu Rev Pharmacol Toxicol*, 47: 143-83.

- Padmavathy, N. and R. Vijayaraghavan. 2008. "Enhanced bioactivity of ZnO nanoparticles-an antimicrobial study". *Science and Technology of Advanced Materials*, 9(3).
- Pasupuleti, S., S. Alapati, S. Ganapathy, G. Anumolu, N. R. Pully and B. M. Prakhya. 2011. "Toxicity of zinc oxide nanoparticles through oral route". *Toxicol Ind Health*.
- Roy, R., A. Tripathi, M. Das and P. D. Dwivedi. 2011. "Cytotoxicity and uptake of zinc oxide nanoparticles leading to enhanced inflammatory cytokines levels in murine macrophages: comparison with bulk zinc oxide". *J Biomed Nanotechnol*, 7(1): 110-1.
- Salata, O. 2004. "Applications of nanoparticles in biology and medicine". *J Nanobiotechnology*, 2(1): 3.
- Sanvicens, N. and M. P. Marco. 2008. "Multifunctional nanoparticles--properties and prospects for their use in human medicine". *Trends Biotechnol*, 26(8): 425-33.
- Sasidharan, A., P. Chandran, D. Menon, S. Raman, S. Nair and M. Koyakutty. 2011. "Rapid dissolution of ZnO nanocrystals in acidic cancer microenvironment leading to preferential apoptosis". *Nanoscale*, 3(9): 3657-69.
- Schwentker, A., Y. Vodovotz, R. Weller and T. R. Billiar. 2002. "Nitric oxide and wound repair: role of cytokines?". *Nitric Oxide*, 7(1): 1-10.
- Sharma, V., D. Anderson and A. Dhawan. 2012. "Zinc oxide nanoparticles induce oxidative DNA damage and ROS-triggered mitochondria mediated apoptosis in human liver cells (HepG2)". *Apoptosis*.

Sohaebuddin, S. K., P. T. Thevenot, D. Baker, J. W. Eaton and L. P. Tang. 2010. "Nanomaterial cytotoxicity is composition, size, and cell type dependent". *Particle and Fibre Toxicology*, 7.

Song, W., J. Zhang, J. Guo, F. Ding, L. Li and Z. Sun. 2010. "Role of the dissolved zinc ion and reactive oxygen species in cytotoxicity of ZnO nanoparticles". *Toxicol Lett*, 199(3): 389-97.

Sun, Z. H., B. Zhao and J. R. Lombardi. 2007. "ZnO nanoparticle size-dependent excitation of surface Raman signal from adsorbed molecules: Observation of a charge-transfer resonance". *Applied Physics Letters*, 91(22).

Tavares Murta, B. M., J. S. Machado, M. Zaparoli, V. C. Lara and E. F. Murta. 1999. "The relationship of host immune cells, cytokine and nitric oxide production to tumor cells in ovarian carcinoma". *Sao Paulo Med J*, 117(2): 87-92.

Valko, M., D. Leibfritz, J. Moncol, M. T. Cronin, M. Mazur and J. Telser. 2007. "Free radicals and antioxidants in normal physiological functions and human disease". *Int J Biochem Cell Biol*, 39(1): 44-84.

Xia, T., M. Kovoichich, M. Liang, L. Madler, B. Gilbert, H. Shi, J. I. Yeh, J. I. Zink and A. E. Nel. 2008. "Comparison of the mechanism of toxicity of zinc oxide and cerium oxide nanoparticles based on dissolution and oxidative stress properties". *ACS Nano*, 2(10): 2121-34.

Yanagisawa, R., H. Takano, K. Inoue, E. Koike, T. Kamachi, K. Sadakane and T. Ichinose. 2009. "Titanium dioxide nanoparticles aggravate atopic dermatitis-like skin lesions in NC/Nga mice". *Exp Biol Med (Maywood)*, 234(3): 314-22.

Yang, H., C. Liu, D. Yang, H. Zhang and Z. Xi. 2009. "Comparative study of cytotoxicity, oxidative stress and genotoxicity induced by four typical

nanomaterials: the role of particle size, shape and composition". *J Appl Toxicol*, 29(1): 69-78.

Yeh, T. K., J. K. Chen, C. H. Lin, M. H. Yang, C. S. Yang, F. I. Chou, J. J. Peir, M. Y. Wang, W. H. Chang, M. H. Tsai, H. T. Tsai and P. Lin. 2012. "Kinetics and tissue distribution of neutron-activated zinc oxide nanoparticles and zinc nitrate in mice: effects of size and particulate nature". *Nanotechnology*, 23(8): 085102.

Zhang, H., B. Chen, H. Jiang, C. Wang, H. Wang and X. Wang. 2011. "A strategy for ZnO nanorod mediated multi-mode cancer treatment". *Biomaterials*, 32(7): 1906-14.

Zhang, L., F. X. Gu, J. M. Chan, A. Z. Wang, R. S. Langer and O. C. Farokhzad. 2008. "Nanoparticles in medicine: therapeutic applications and developments". *Clin Pharmacol Ther*, 83(5): 761-9.

Zheng, Y. F., R. Z. Li and Y. D. Wang. 2009. "In Vitro and in Vivo Biocompatibility Studies of ZnO Nanoparticles". *International Journal of Modern Physics B*, 23(6-7): 1566-1571.